Photofragmentation of Acetyl Cyanide at 193 nm

Ronald J. Horwitz,[†] Joseph S. Francisco,*[,‡] and Joyce A. Guest*[,†]

Department of Chemistry, University of Cincinnati, Cincinnati, Ohio 45221-0172, and Department of Chemistry and Department of Earth and Atmospheric Sciences, Purdue University, West Lafayette, Indiana 47907-1393

Received: November 14, 1996[⊗]

The photodissociation of gaseous acetyl cyanide has been examined following excitation at 193 nm. CN $X^2\Sigma^+$ photofragments were probed via laser fluorescence excitation to determine their rotational, vibrational, and translational energy distributions. CN was produced in $v'' = 0$ and 1 with mean rotational energy (13.5 ± 2) kJ mol^{-1}, and $v'' = 2$ with mean rotational energy (10 ± 4) kJ mol^{-1}. Mean translational energies of the CN fragments were (32 ± 10) kJ mol^{-1}. Ab initio electronic structure theory has been used to characterize the heat of formation for acetyl cyanide along with its geometries and vibrational frequencies. The acetyl cyanide heat of formation, $\Delta H^0_{f,0}$, is predicted to be (−0.4 ± 8) kJ mol^{-1} using Gaussian-2 theory (G2). The theoretical results are used to compute bond dissociation energies of acetyl cyanide for further interpretation of the experimental photodissociation data. Evidence is presented that the majority of CN fragments are produced via dissociation of the parent acetyl cyanide to CH_3CO + CN, with subsequent decomposition of the acetyl fragment. The alternate possible primary α-cleavage pathway to CH_3 + OCCN is proposed as a possible source for the OCCN radical.

Introduction

Studies of medium-sized carbonyl compound α-cleavage dynamics have contributed insights into the mechanisms and pathways of a series of related photodissociation processes. Compounds such as acetone[1,2] and acetic acid[3,4] are observed to dissociate to translationally energetic fragments following sufficiently energetic electronic excitation. Photofragment energy distribution details are consistent with assertions that such primary α-cleavage processes proceed via electronic surface crossing mechanisms that include an exit channel barrier. Previous work from this group has demonstrated that the stronger of the two bonds adjacent to the carbonyl group can break in high yield, counter to the then-held expectation that the weaker of the two α-bonds would break preferentially following $^1(n,\pi^*)$ electronic excitation. Another family of carbonyl compounds, the acetyl halides,[5] lose their α-halogens rapidly and selectively, apparently via adiabatic dynamics that differ quantitatively from first-row carbonyl dissociation dynamics.

We present here the first report of the photodissociation of acetyl cyanide, a carbonyl compound containing a multiply bonded substituent. The photofragmentation pathways and dynamics of acetyl cyanide could well be different from those of the family of much-studied carbonyl compounds containing first-row substituents. Conjugation in acetyl cyanide might result in atypical photochemical pathways. Electron delocalization affects the C−CN bond, reducing the bond length from that of a typical single bond. The same −CN substituent causes the lowest singlet excited electronic state to be red-shifted significantly with respect to acetone.[6,7]

The excited electronic states and the photochemistry of acetyl cyanide have seen surprisingly little attention to date, both experimentally[6] and theoretically.[8] Electronic excitation of acetyl cyanide at 193 nm accesses a state above S_1 that is presently unassigned. The corresponding band in similar carbonyl compounds[9,10] is assigned to $^1(n,3s)$ Rydberg excitations; molecules excited to these levels subsequently predissociate from a lower electronic surface. To our knowledge, there have been no previous reports of acetyl cyanide photochemistry in any spectral region. In the present work, we begin to evaluate the possible photodissociation pathways and dynamics of acetyl cyanide by examining energetic details of the CN photofragment.

To assess the possible photochemistry of acetyl cyanide, it is necessary to know the heat of formation of this species. There have been no experimental reports of the acetyl cyanide heat of formation to this time. In the present work, ab initio molecular orbital methods are used to examine the energetics of acetyl cyanide; formyl cyanide is used to calibrate the energetics. The heat of formation of acetyl cyanide is predicted reliably, and the dissociation threshold for the C−CN bond cleavage process is determined.

We also present here the first report of ab initio calculations of acetyl cyanide structural properties employing electron correlation. Structural determinations of gaseous acetyl cyanide began with the 1959 report of Krisher and Wilson[11] and have continued with gas-phase electron diffraction work,[12] further spectroscopic studies,[13−15] and the evaluation of vibrational frequencies from ab initio calculations using Hartree−Fock wave functions.[15] An interesting aspect of the acetyl cyanide structure is the electron delocalization across this species' C−CN bond which perturbs the C−CN bond length and bond strength significantly from the typical single-bond character. Such C−CN bond strength perturbation increases the expected dissociation threshold for the process $CH_3COCN \rightarrow CH_3CO$ + CN over that expected for single C−C bond fission.

Experimental Section

The basic experimental arrangement has been described in detail previously.[3] In the present study, a low-pressure flowing gas sample of acetyl cyanide was photolyzed at 193 nm, and the CN photofragments that resulted were studied using laser excited fluorescence.

The reaction chamber, a 30 cm aluminum cube with baffle arms, was evacuated with a mechanical pump through a liquid

* Authors for correspondence.
[†] University of Cincinnati.
[‡] Purdue University.
[⊗] Abstract published in *Advance ACS Abstracts,* January 15, 1997.

S1089-5639(96)03800-5 CCC: $14.00

nitrogen trap. Acetyl cyanide samples ("pyruvonitrile", Aldrich, 95%) were subjected to several freeze−pump−thaw cycles and held in darkened glass sample containers. Acetyl cyanide hydrolysis by water was prevented by eliminating all traces of water from sample lines. The acetyl cyanide was flowed through the reaction chamber at a rate equivalent to replacing the chamber volume every 10−20 s at the chamber sample pressure of 10−20 mTorr. The acetyl cyanide was photolyzed with the 193 nm light from an ArF excimer laser (Lambda Physik, EMG103MSC). Photolysis laser light passed through an iris and was mildly converged with a 1 m focal length lens into the interaction region to energy densities not greater than about 1 mJ cm^{-2}. The counterpropagating probe laser for the CN $B^2\Sigma^+ - X\ ^2\Sigma^+$ ($\Delta v = +1$) sequence bands in the 354−359 nm region was held to an energy density of 35−70 μJ cm^{-2} to minimize saturation effects.[16] Fluorescence emission was observed from the 193 nm excitation of the acetyl cyanide sample and could be due to parent fluorescence or impurity fluorescence. This signal was minimized by delaying the probe laser pulse by 300 ns from the photodissociation laser rising edge.

The CN B−X fluorescence signal was collected by *f*/1 optics, imaged onto a slit, filtered to reduce scattered light, and detected by a photomultiplier tube/gated integrator combination. Photolysis and probe laser powers were monitored and stored to normalize the fluorescence signal for laser intensity variations.

Rotationally and translationally thermalized CN samples were produced by photolyzing mixtures of 15 mTorr of acetyl cyanide with 9 Torr of argon gas, and delaying the probe laser to 2.2 μs after the photolysis laser. These thermalized samples were used to verify the photofragment rotational distribution analysis and for photofragment Doppler broadening measurements.

Computational Methods

All calculations are performed using the GAUSSIAN 92 program.[17] Geometry optimizations are carried out for all structures using Schlegel's method,[18] to better than 0.001 Å for bond lengths and 0.1° for angles, with a self-consistent field convergence of at least 10^{-9} on the density matrix. The residual rms force is less than 10^{-4} au. The optimizations are performed at the Hartree−Fock and second-order Møller−Plesset (MP2) level of theory, with the medium split-valence 6-31G(d) basis set. This basis set is enlarged by supplementing them with additional sets of polarization functions on all the heavy atoms and the hydrogens, to make up the 6-311G(2d,2p) basis set. A set of f-polarization functions and an extra set of d-polarization functions are added to comprise the 6-311G(3df,3pd) basis set. Vibrational frequencies are calculated analytically at the MP2/6-31G(d) and MP2/6-311G(2d,2p) level of theory. Heats of formation are calculated using G2 theoretical procedures. The G2 method is a composite one, based on the optimization of structures at the MP2/6-31G(d) level, followed by single-point calculations at higher levels of theory, leading to a final predicted total energy. These methods[19,20] have been tested on a series of molecules having well-established experimental values for their dissociation energies, which are accurate to within ±8 kJ mol^{-1}.

Results and Discussion

CN Photofragment Distributions. Figure 1 shows the R branch of the B−X ($\Delta v = +1$) fluorescence excitation spectrum of CN $X^2\Sigma^+$ photofragments resulting from the 193 nm dissociation of acetyl cyanide, normalized for pump-and-probe laser powers. The CN line positions were assigned by reference to published assignments and spectral constants.[21] Appropriate

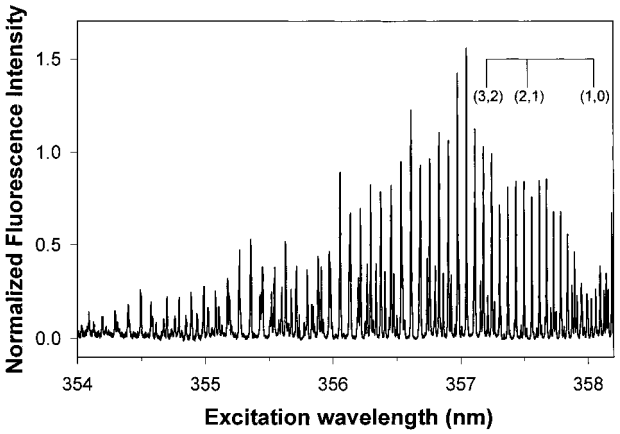

Figure 1. CN B−X ($\Delta v = +1$) fluorescence excitation spectrum following 193 nm dissociation of acetyl cyanide. Spectrum is normalized for photolysis and probe laser powers. Band origin positions are indicated.

Hönl−London factors[22] and Franck−Condon factors[23] were used to extract relative rotational and vibrational populations from the intensity data. The spectrum shows evidence of significant vibrational excitation; rovibrational transitions from $v'' = 0$, 1, and 2 are discernible, leading to some spectral congestion. No transitions from $v'' = 3$ could be unambiguously assigned. Only nonoverlapping transitions were selected for further analysis.

In the present study, spectral line splitting resulting from N''-dependent spin−rotation doubling effects became observable beginning at about $N'' = 13$ in $v'' = 0$, 1, and 2. The effects of level-dependent line doubling were included in the general population extraction procedure. Relative rotational populations for $v'' = 0$, 1, and 2 extracted from the photofragment CN R-branch data are shown in Figure 2. The population axis magnitudes are scaled so that the rotational populations can be compared among the three vibrational levels. The populations in $v'' = 0$ and 1 are fit well for all but the lowest values of N'' by a Boltzmann distribution with a single temperature parameter. Rotational populations in $v'' = 2$ exhibit significant scatter, so the approximation of a single Boltzmann distribution is uncertain compared to the lower v'' states. The solid lines in each graph of Figure 2 are the rotational distributions corresponding to the temperature that best fits the experimental data. All three rotational temperatures are the same to within the experimental uncertainty, approximately 1800 K. These temperatures imply not true equilibrium but rather a useful parametric model to the observations.

The measured and fitted rotational populations were utilized along with the appropriate Franck−Condon factors to evaluate the relative vibrational populations in CN $X^2\Sigma^+$ ($v'' = 0$, 1, and 2). The resulting v'' = 0:1:2 population ratio is approximately 1.0:0.21:0.04, or 80% in $v'' = 0$, 17% in $v'' = 1$, and 3% in $v'' = 2$. The relative vibrational populations fit well to a Boltzmann distribution of $T \approx 1800$ K, the same as the rotational temperature parametrization.

We observed a reproducible line broadening of the CN photofragment rovibronic transitions compared to those for the corresponding thermalized samples. The rotationally thermalized CN samples were reasonably expected to be translationally thermalized to 300 K as well, so we attributed the photofragment line broadening to Doppler broadening[24] from the translationally energetic fragments. The profiles for several B−X (1,0) transitions of the 300 K CN were modeled empirically by a convolution of Lorentzian line profiles having mean full width at half-maximum (fwhm) 0.24 ± 0.02 cm^{-1} with the Doppler

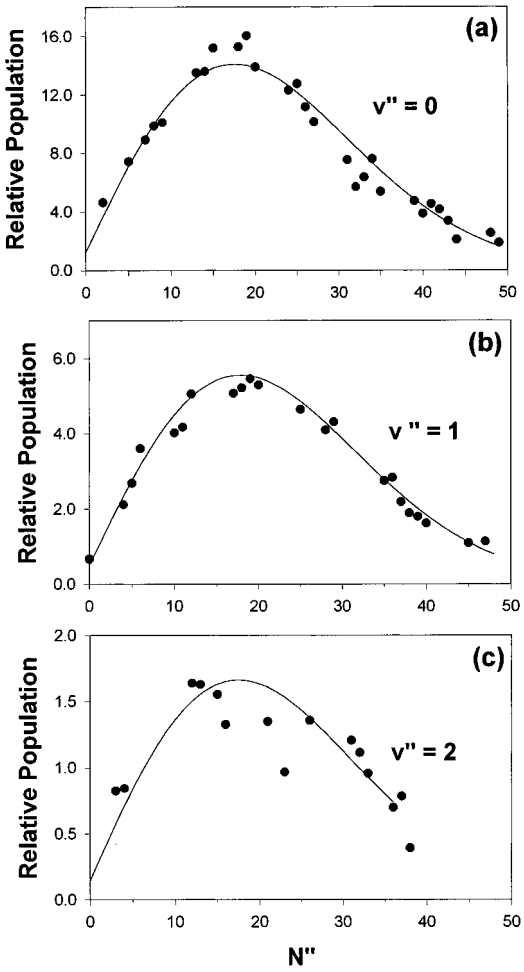

Figure 2. CN $X^2\Sigma^+$ fragment populations in $v'' = 0$, 1, and 2 (closed circles). Mean uncertainty (1σ) is ±10% for $v'' = 0$, 1 and ±20% for $v'' = 2$. Solid lines show populations predicted for best-fit single temperature parameters.

profile corresponding to a 300K CN sample. The Lorentzian profile was then taken to approximate the probe laser's instrumental line shape and used for further analysis. Several CN photofragment B−X (1,0) and (2,1) transitions, ranging from R(2) to R(49), were examined to evaluate best-fit line profiles. Figure 3 shows the model results for a representative transition of thermalized and photofragment CN. Gaussian profiles of average fwhm 0.20 ± 0.03 cm^{-1} (1σ uncertainty), when convoluted with the instrument function Lorentzian profile and a Gaussian profile corresponding to parent motion, yielded the best fits to the series of photofragment line profiles. This photofragment line profile corresponds to a sample of CN molecules with translational $T = 2600 \pm 800$ K and a mean translational energy $\bar{E}_T$ of 32 ± 10 kJ mol^{-1}.

Table 1 summarizes the CN $X^2\Sigma^+$ photofragment mean rotational ($\bar{E}_R$), vibrational ($\bar{E}_v$), and translational ($\bar{E}_T$) energies. Only rotational states up to the maximum state measured experimentally were included in the $\bar{E}_R$ and $\bar{E}_v$ analyses. The mean vibrational energy includes contributions only from the observed $v'' = 0$, 1, and 2 states. The quoted translational energy involves the evaluation of several representative Doppler-broadened lines in both $v'' = 0$ and $v'' = 1$ of CN.

Theory: Acetyl Cyanide Thermochemistry. The heat of formation for acetyl cyanide is estimated using G2 theory. We compare this to a calculation at the G2 level for formyl cyanide to explore the reliability of both sets of calculations. The G2 energetics for both molecules are listed in Table 2. From the heats of formation, it can be readily seen that acetyl cyanide is

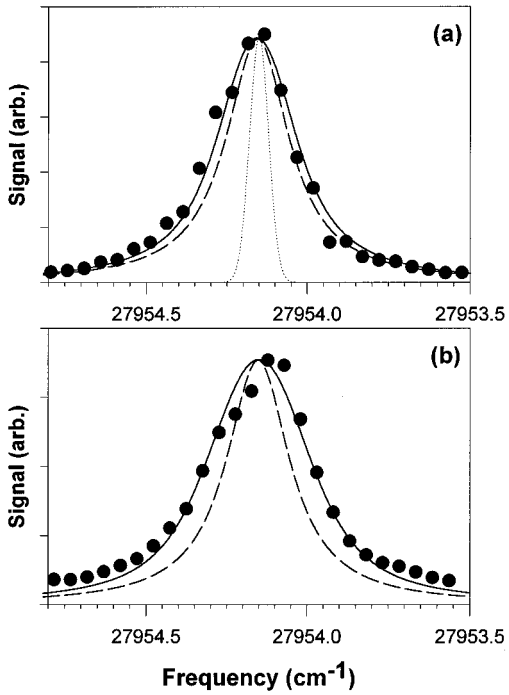

Figure 3. Experimental fluorescence excitation line profiles and model profiles for (1,0) R(5) CN B−X transition for (a) thermalized and (b) photofragment. In (a) and (b), dashed line is laser line profile (0.24 cm Lorentzian profile) and solid line is convolution fit to experiment (closed circles). In (a), dotted line represents 300 K Doppler profile for CN.

TABLE 1: CN $X^2\Sigma^+$ Photofragment Mean Energies (kJ mol^{-1})

v''	rotation	vibration	translation
0	13.5 ± 2	5.6 ± 0.5	32 ± 10
1	13.5 ± 2		
2	10 ± 4		

TABLE 2: Acetyl and Formyl Cyanide G2 Energetics

acetyl cyanide	
total energy (hartrees)	−245.685 97
atomization energy (kJ mol^{-1})	3499.9
$\Delta H°_{f,0}$ (kJ mol^{-1})	−0.4
$\Delta H°_{f,298}$ (kJ mol^{-1})	−15
formyl cyanide	
total energy (hartrees)	−206.447 57
atomization energy (kJ mol^{-1})	2307.5
$\Delta H°_{f,0}$ (kJ mol^{-1})	48.5

thermodynamically more stable than formyl cyanide. This is consistent with experimental observations. The formyl cyanide heat of formation of 48.5 kJ mol^{-1} (G2) seem reasonable when we compare it to the heat of formation obtained from calculating it by the bond separation energy (BSE) method. In this case the simple reaction is the separation of formyl cyanide into its simplest fragment molecules:

$$HCOCN \rightarrow HCO + CN$$

This approach is generally not as accurate as the G2 method, and it has an uncertainty of ±17 kJ mol^{-1}, even in the best case. Nevertheless, it does provide another avenue to check the reliability of the G2 results. From the calculated $D°$(C−CN) for formyl cyanide, along with the experimental heats of formation of HCO[25] of 43.1 ± 10.5 kJ mol^{-1} and CN[26] of 435.6 ± 2.1 kJ mol^{-1}, the heat of formation of formyl cyanide is estimated as 45.6 kJ mol^{-1} using G2 in the BSE scheme. The heat of formation of formyl cyanide calculated from G2 and

TABLE 3: C−CN Bond Dissociation Energy (kJ mol^{-1})

species	method	$D°$(C−C≡N)	ref
CH_3COCN	G2	425.9	this work
	MP3/6-31++G**	438.5	29
HCOCN	G2	430.1	this work
	BSE (G2)	433.0	this work
	MP4/6-31G*//HF/6-31G*	496.2	28
CH_2═CH_2		715.5 ± 5.0	
CH_3−CH_3		368.2 ± 8	

by the bond separation energy (BSE) methods agree within 2.9 kJ mol^{-1}, which is within the range of expected errors for the two methods. As a further check of the G2 results, an estimate of the heat of formation of formyl cyanide was obtained from the isodesmic reaction:

$$HCOCN + HCN \rightarrow CH_2O + C_2N_2$$

given the heats of formation for HCN, CH_2O, and C_2N_2 of 135.6 ± 8, −112.056 ± 6.3, and 311.3 ± 2.1 kJ mol^{-1}, respectively; and also given that at the QCISD(T)/6-311G(3df,3pd) level the heat of reaction is estimated as 17.6 kJ mol^{-1}. This yields an estimate for the heat of formation of 38 kJ mol^{-1}, which is in reasonable agreement with the G2 heat of formation determination. These results suggest that the heats of formation for acetyl cyanide predicted using the G2 method should be reliable.

The CC bond lengths in formyl cyanide (r(C−CN) = 1.473 Å) and acetyl cyanide (r(C−CN) = 1.483 Å) suggest that the CC bond dissociation energies ($D°$(C−CN)) for these species are similar. The experimental heat of formation of the acetyl radical[27] of 10.0 ± 1.2 kJ mol^{-1} and of CN of 435.6 ± 2.1 kJ mol^{-1} can be used with the heat of formation of acetyl cyanide to determine its C−C bond dissociation energy (see Table 3). The CC bond energy is 430.1 and 425.9 kJ mol^{-1} for formyl and acetyl cyanide, respectively, from G2 results. There is good consistency between G2 and BSE bond dissociation energies for the CC bond for formyl cyanide. The only other estimate of the C−CN bond dissociation energy comes from calculations of Fang et al.,[28] who estimated a value of 496.2 kJ mol^{-1} at the MP4/6-31G*//HF/6-31G* level of theory, which leads to a value for the heat of formation of formyl cyanide of −17.6 kJ mol^{-1}. This suggests that formyl cyanide is thermodynamically more stable than acetyl cyanide, which is inconsistent with experimental observation. The problem with the result of Fang et al.[28] lies in the fact that the basis set used is too small, and the electron correlation used is too modest to provide the best estimate of the dissociation limit. As an illustration of this point, we estimated the $D°$(C−CN) for formyl cyanide at the MP2/6-311G(2d,2p) level and obtained a result consistent with Fang et al.,[28] i.e., 512.1 kJ mol^{-1}. We find that high levels of electron correlation and large basis sets are needed to converge the energies in order to obtain reasonable results.

The C−C bond dissociation energy for acetyl cyanide is consistent with the earlier estimate of Wiberg and co-workers[29] obtained from the MP3/6-31++G** level of theory. (Given the problem with formyl cyanide with the smaller basis set and modest electron correlation, the MP3/6-31++G** result of Wiberg and co-workers could be fortuitous.) Comparing $D°$(C−CN) for formyl and acetyl cyanide shows that their bond dissociation energies are quite similar, as the CC bond lengths suggest. Comparing the $D°$(C−CN) for the cyanides to that in ethylene of 715.5 ± 5.0 kJ mol^{-1} and to ethane of 368 ± 8 kJ mol^{-1} suggests that the C−CN bond in acetyl cyanide exhibits some double-bond character, but not a significant amount. Also from the structural data, it could be seen that conjugative effects across the C−CN bond is reduced by methyl substitution. This suggests that the C−CN bond should exhibit more single and less double-bond character. As a result, one would expect the $D°$(C−CN) in acetyl cyanide to be slightly less than that in formyl cyanide. From G2 results, the acetyl cyanide $D°$(C−CN) is 4 kJ mol^{-1} less than the $D°$(C−CN) in formyl cyanide, which is consistent with the structural trends.

Theory: Acetyl Cyanide Geometry and Frequencies. The ab initio and experimental acetyl cyanide bond lengths and angles are presented in Table 4. The theoretical bond lengths agree with the experimental bond lengths[12] to within 1.5% (rms), and the bond angles agree to within 0.6%. This suggests that the MP2/6-311G(3df,3pd) results are reasonable. It is interesting to note that the molecular constants for acetyl cyanide are in good agreement with the experimental microwave[11] data (see Table 5).

A noteworthy feature of the acetyl cyanide structure is the C−C bond. At the MP2/6-311G(3df,3pd) level of theory, the C−C bond length is predicted to be 1.483 Å for acetyl cyanide Recall that in ethane, the C−C bond is a single bond of length 1.543 ± 0.003 Å. In ethylene and acetylene, the C−C bond is a double (1.339 ± 0.002 Å) and triple (1.204 ± 0.002 Å) bond, respectively. The C−C bond in acetyl cyanide appears to exhibit some double-bond characteristics. The C−CN bond character of acetyl cyanide seems similar to that in propynal (HCOCCH)[30] and formyl ethylene ($HCOCHCH_2$),[31] where the C−C bond lengths are 1.453 and 1.484 Å, respectively. It appears that the methyl substitution lessens the conjugative effects across the C−CN bond in acetyl cyanide.

For acetyl cyanide, there are eighteen normal vibrational modes, which transform under the symmetry operation of the C_s point group as

$$\Gamma = 12a' \oplus 6a''$$

TABLE 4: Geometries for Acetyl Cyanide (Å and degrees)

		level of theory			
species	coordinate	MP2/6-31G(d)	MP2/6-311G(2d,2p)	MP2/6-311G(3df,3pd)	expt[a]
CH_3COCN	C′N	1.182	1.171	1.169	1.167 ± 0.010
	CC′	1.480	1.483	1.474	1.477 ± 0.008
	CC	1.499	1.497	1.493	1.518 ± 0.009
	CO	1.223	1.211	1.207	1.208 ± 0.009
	CH	1.094	1.087	1.089	1.116 ± 0.011
	CH′	1.090	1.082	1.084	
	CCC	115.3	114.9	114.7	114.2 ± 0.9
	CC′N	179.8	179.8	179.1	179.2 ± 2.2
	CCO	125.2	125.3	125.4	124.6 ± 0.7
	OCC′	119.5	119.7	119.9	
	HCC	109.9	109.6	109.7	
	H′CC	109.1	109.5	109.4	

[a] Reference 12.

TABLE 5: Molecular Constants (in MHz) for acetyl cyanide

species	constants	MP2/6-311G(3df,3pd)	expt
CH_3COCN	A	10243.8	10185.46[a]
	B	4164.5	4157.53
	C	3015.5	3002.75

[a] Reference 11.

All of these vibrational modes are infrared active. Theoretical and experimental vibrational frequencies and their assignments are given in Table 6. Bell et al.[15] reported vibrational frequencies calculated at the Hartree−Fock level with 3-21G, 6-31G, and DZ basis sets. The rms error between calculated vibrational frequencies at HF/DZ level is 16.9%. The present vibrational frequencies calculated at the MP2/6-311G(2d,2p) level show better agreement, with an rms error of 5.6%.

Photochemical Reaction Pathway Evaluation. We have determined the rotational, vibrational, and translational energy distributions of the CN fragment produced via photolysis of acetyl cyanide. Interpretation of these results is hampered by the dearth of experimental information on the thermochemistry of acetyl cyanide and one of its possible fragments, OCCN. The present theoretical calculations provide a useful $\Delta H°_{f,298}$ for acetyl cyanide (Table 2), and a 0 K C−CN bond dissociation energy (Table 3) that is significantly stronger than a typical C−C single bond. This C−CN bond dissociation energy agrees well with an evaluation using a combination of the ab initio enthalpy of formation and available experimental enthalpies, and it is used in the following discussion.

The possible pathways by which the observed CN photofragment could be formed following excitation of room-temperature acetyl cyanide with 193 nm (619 kJ mol^{-1}) light are[25−27]

$$CH_3COCN \rightarrow CH_3CO + CN \qquad (\Delta H° = 427 \text{ kJ mol}^{-1}) \tag{1}$$

or

$$CH_3COCN \rightarrow CH_3 + OCCN \tag{2a}$$

followed by

$$OCCN \rightarrow CO + CN \qquad (\text{overall } \Delta H° = 485 \text{ kJ mol}^{-1}) \tag{2b}$$

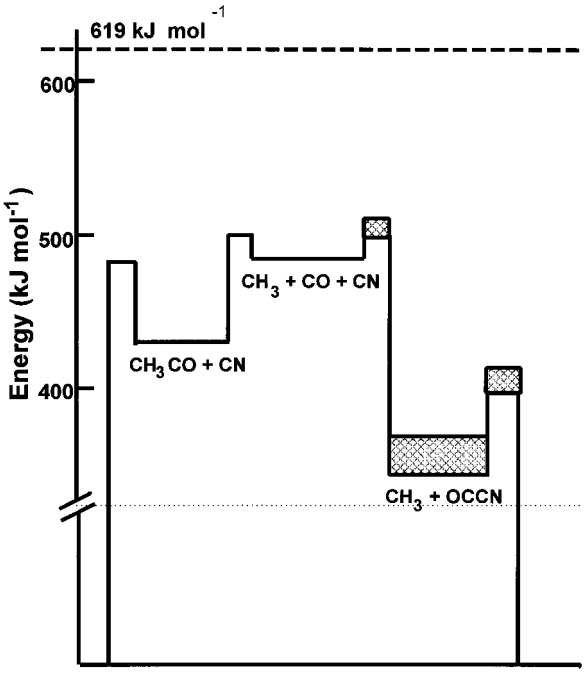

Figure 4. Energetically possible reaction paths to produce CN from acetyl cyanide photolysis at 193 nm (∼619 kJ mol^{-1}).

Figure 4 shows the energetics of the various reaction pathways by which the CN fragment can be produced following deposition of ∼619 kJ mol^{-1} (193 nm light) into acetyl cyanide molecules. Both thermochemical and estimated dissociation barriers are included. Crosshatching indicates energies of high uncertainty because the OCCN $\Delta H_f°$ is unknown. Figure 4 will be used for the following discussion.

Considering only thermochemistry, there should be ample energy deposited at 193 nm to effect dissociation to CH_3 + CO + CN via single-photon absorption. However, a well-established pattern of observations justifies that primary α-cleavage of simple first-row gas-phase carbonyls occurs following passage over an exit barrier of average energy 54−58 kJ mol^{-1}; therefore, exit barriers will be included here. We propose that such barriers operate for both the pathway to CH_3CO + CN and the pathway to CH_3 + OCCN.

If acetyl cyanide dissociates to acetyl and CN fragments, then our experiments measure photofragments from a primary dissociation process. If all of the presumed exit barrier of ∼56

TABLE 6: Vibrational Frequencies (in cm^{-1}) for Acetyl Cyanide

species	mode no.	mode sym	mode description	frequencies MP2/6-31G(d)	frequencies MP2/6-311G(2d,2p)	expt[a]
CH_3COCN	1	a′	CH3 antisym stret.	3240	3222	3027
	2		CH_3 sym stret.	3111	3095	2932
	3		C′N stret	2184	2154	2229
	4		CO stret	1763	1743	1740
	5		CH_3 antisym bend	1523	1488	1431
	6		CH_3 sym bend	1450	1416	1368
	7		CC′ stret	1243	1215	1178
	8		CH_3 in-plane rock	1020	998	976
	9		CC stret	738	722	712
	10		CCC′ bend	597	590	584
	11		CCO bend	436	431	431
	12		CC′N bend	172	170	176
	13	a″	CH_3 antisym stret	3195	3174	2476
	14		CH_3 antisym bend	1526	1496	1428
	15		CH_3 rock	1077	1056	1026
	16		CO wag	606	591	535
	17		CC N bend	260	247	245
	18		CH_3 torsion	140	144	(126)

[a] Reference 15.

kJ mol^{-1} partitions into fragment translational degrees of freedom, then 136 kJ mol^{-1} remains for partitioning among fragment rotational and vibrational degrees of freedom. The present results indicate the CN average rotational energies $\bar{E}_{R(v'')}$, are approximately 15 kJ mol^{-1} in $v'' = 0$, 1, and 2, and average vibrational energy $\bar{E}_v$ over zero-point is about 5.5 kJ mol^{-1}. This leaves on average 116 kJ mol^{-1} for internal energy of the acetyl, ample to surmount its 71 kJ mol^{-1} dissociation barrier[32] to $CH_3 + CO$. We will draw the analogy from the well-studied photochemistry of acetone at 193 nm that this dissociation to three fragments is likely a stepwise, uncorrelated process.

The real complication for the present experimental interpretation is that an important dissociation pathway might be step 2a, $CH_3 + OCCN$, followed by secondary dissociation of the OCCN to give the CN fragments that we monitor. The likelihood of such a fragmentation pathway will now be considered, following the procedure outlined by Hunnicutt et al.[4] for acetic acid photochemistry at 200 nm. We begin by assuming a mean exit barrier of 56 kJ mol^{-1} for the dissociation to $CH_3 + OCCN$, all channeled into translation. Momentum conservation requires that the methyl fragment acquires 43 kJ mol^{-1} in translation, and OCCN acquires 13 kJ mol^{-1} in translation. Our experimental estimate for $\bar{E}_T$(CN) is 32 kJ mol^{-1}; if the two-step pathway 2a and 2b operates, the observed CN translation is acquired from both the primary (step 2a) and secondary (step 2b) dissociations. Given that steps 2a and 2b are uncorrelated, that is, OCCN rotates sufficiently prior to dissociation to be isotropically distributed relative to the velocity v(OCCN) from step 2a, then

$$v^2(\mathrm{CN}) = v^2(\mathrm{OCCN}) + w^2(\mathrm{CN})$$

$$v^2(\mathrm{CO}) = v^2(\mathrm{OCCN}) + w^2(\mathrm{CO})$$

where v^2 is the mean-square velocity relative to the parent center-of-mass frame, and w^2 is the mean square velocity relative to the fragment OCCN center of mass. Including linear momentum conservation for step 2b, $m(\mathrm{CO})\boldsymbol{w}(\mathrm{CO}) = -m(\mathrm{CN})\boldsymbol{w}(\mathrm{CN})$, we find that $\bar{E}_T(\mathrm{CO}) = 31$ kJ mol^{-1}. Thus, for dissociation pathway (2) leading to three fragments, the mean translational energy of all three fragments $\bar{E}_T(\mathrm{total}) = \bar{E}_T(\mathrm{CH_3}) + \bar{E}_T(\mathrm{CO}) + \bar{E}_T(\mathrm{CN}) = 106$ kJ mol^{-1}, given (1) primary α-cleavage in step 2a with a 56 kJ mol^{-1} exit barrier, (2) uncorrelated secondary recoil for step 2b, (3) experimental $\bar{E}_T(\mathrm{CN}) \approx 32$ kJ mol^{-1}. Using the quoted uncertainty in the mean $\bar{E}_T$(CN), the $\bar{E}_T$(TOTAL) can range from 86 to 125 kJ mol^{-1}.

Thermochemistry indicates that about 134 kJ mol^{-1} of energy is available for partitioning into all fragment translational, vibrational, and rotational degrees of freedom following dissociation to three fragments. Partitioning 106 kJ mol^{-1} of that energy into translation leaves only 28 kJ mol^{-1} to distribute among the CH_3, CO, and CN fragment vibrational and rotational degrees of freedom. While our argument is not unequivocal, it provides evidence that CN from pathway (2) is a minority species in the present study. The translational recoil model on which the present argument is based led us to predict that an acetic acid dissociation pathway to $CH_3 + OCOH$ would ultimately yield a stable OCOH radical.[4] This prediction was subsequently demonstrated experimentally when Sears and coworkers[33] discovered that acetic acid photolyzed at 193 nm produced the OCOH radical in measurable yield. The following discussion of the dissociation dynamics will consider CN as the primary photofragment.

Dissociation Dynamics. A primary dissociation process via the pathway described by step (1) leaves 192 kJ mol^{-1} to partition among the various acetyl and CN degrees of freedom. When we include the mean translational recoil and the vibrational and rotational energies, there remains ample excess energy for the acetyl fragments to dissociate. Therefore, acetyl fragments are not expected to survive the overall dissociation process intact. Their fate, however, is not observed in the present experiments.

The acetyl cyanide excited state initially accessed by 193 nm radiation is unassigned at present. The spectroscopy of the first singlet electronic excitation, a singlet n → π* band, has been studied by room-temperature absorption and jet-cooled fluorescence excitation and will be presented in a future publication.[7] 193-nm light accesses a strongly allowed transition, which by analogy to acetone and acetaldehyde spectroscopy is probably a ^{1}(n,3s) Rydberg band. Related studies of acetone photolysis via ^{1}(n,π*) and ^{1}(n,3s) excitations indicate that the dissociation mechanism following each excitation involves surface crossing to a lower electronic state and subsequent exit barrier traversal.[1,10] The acetone dissociation to $2CH_3 + CO$ requires about 80% of the energy required to dissociate acetyl cyanide to $CH_3 + CO + CN$; therefore, 193 nm excitation of acetone releases nearly 100 kJ mol^{-1} more energy to three fragments than does the 193 dissociation of acetyl cyanide into three fragments.

The results presented in Table 1 show that only about 35% of the available energy following dissociation to $CH_3CO + CN$ appears in the CN X state photofragment rotation and vibration, and both fragments' translation. Over 120 kJ mol^{-1} remains in the acetyl fragment, ample for dissociation. It is instructive to examine the energy-disposal predictions of two simple dissociation models, one impulsive and one statistical, to acquire some understanding of the primary dissociation mechanism. The direct impulsive dissociation model[34] describes fragment translational and rotational energy partitioning following an impulse imparted to the two immediately separating atoms involved in the bond fission process.

The impulsive model is extremely primitive compared to the complexities of real polyatomic molecule dissociation dynamics, but the model does provide a limiting description to which fragment energy partitioning data may be related. Model results predict that 23% of the available energy following bond dissociation is imparted to CN translation independent of excitation energy (44 kJ mol^{-1} for 193 nm excitation of acetyl cyanide). The predicted $\bar{E}_T$(CN) is at the upper limit of the large uncertainty for our extracted CN mean translational energy. This seeming consistency with impulsive translational energy predictions is probably entirely fortuitous. Photodissociation studies of related compounds acetic acid and acetone over a range of excitation energies have indicated that the primary dissociation fragment translational energies vary little with excitation energy, an observation more indicative of an exit barrier mechanism than a direct impulsive process.

The impulsive model predicts an extremely small mean CN rotational energy content, less than 0.25 kJ mol^{-1}, when the acetyl cyanide ground state near-linear C−C≡N bond geometry is used.[15] The modeled C−C≡N bond angle that corresponds best to our experimental mean rotational energy is 145−150°. This apparent disagreement is not surprising when one considers the complexity of the real dissociation process. First, room-temperature parent acetyl cyanide contains significant low-frequency CCN bending excitation that transforms to product rotation. Of more significance here is that redistribution of excitation energy following crossing to a lower electronic surface should result in substantial high-amplitude vibrational excitation in acetyl cyanide prior to the final bond fission; high CCN in-

plane and out-of-plane bending excitation should lead to substantial rotational excitation in the CN fragment.

A second, statistical dissociation model[35] considers a limit where all final quantum states are equally probable. For dissociation to $CH_3CO + CN$ with all 192 kJ mol^{-1} of available energy, the CN X vibrational distribution ratio for $v'' = 0{:}1{:}2$ is estimated to be 1.0:0.13:0.012, corresponding to an effective temperature of about 1300 K. This result is somewhat less energetic than the experimentally determined vibrational distribution. If we remove the approximately 56 kJ mol^{-1} that would be required to surmount an exit barrier from the available energy, the $v'' = 0{:}1{:}2$ vibrational population ratio becomes 1:0.05:0.001. This is far lower than the experimental vibrational distribution. Thus, if an exit barrier to the dissociation of acetyl cyanide exists as for other similar carbonyl compounds, a statistical model would not explain the results adequately.

A combination of impulsive and statistical models has been presented by North et al.[1] for application to acetone and acetic acid photofragment product distributions at several parent excitation energies. The separate energy reservoirs they invoke account for a nearly constant exit barrier as well as thorough redistribution of the rest of the available energy prior to dissociation. An appropriate application of this model to acetyl cyanide dissociation would require fragment energy distribution data at two or more photolysis energies, information unavailable at this time.

Concluding Remarks

We have presented the first experimental report of the photodissociation of acetyl cyanide via examination of the CN $X^2\Sigma^+$ fragment. The CN fragments contain about 35% of the energy available to the products $CH_3CO + CN$. Fragment CN rotational and vibrational product state distributions are described well by Boltzmann distributions with the same effective temperature. Arguments have been offered to justify that CN is a primary photofragment rather than the result of a secondary dissociation process. An absolute demonstration that the observed CN results from a single chemical pathway is not possible at this time.

The multiple available photochemical pathways for acetyl cyanide, coupled with electron delocalization effects, makes the elucidation of its photochemical dynamics a significant complement to related carbonyls and nitriles. More thorough evaluation of acetyl cyanide photochemistry will require studies that evaluate the first dissociation limit to $CH_3 + OCCN$, and include a spectroscopic search for CN $A^2\Pi$, the production of which is energetically feasible at 193 nm. Finally, acetyl cyanide photolysis is a possible direct source for the still unreported OCCN radical, in much the same way as the acetic acid photolysis pathway to $CH_3 + HOCO$ was discovered to represent a source for the previously elusive HOCO radical.

Acknowledgment. J.A.G. acknowledges research support from the Petroleum Research Fund, administered by the American Chemical Society.

References and Notes

(1) North, S. W.; Blank, D. A.; Gezelter, J. D.; Longfellow, C. A.; Lee, Y. T. *J. Chem. Phys.* **1995,** *102*, 4447.
(2) Waits, L. D.; Horwitz, R. J.; Guest, J. A. *Chem. Phys* **1991**, *155*, 149.
(3) Hunnicutt, S. S.; Waits, L. D; Guest, J. A. *J. Phys. Chem.* **1989**, *93*, 5188.
(4) Hunnicutt, S. S.; Waits, L. D; Guest, J. A. *J. Phys. Chem.* **1991,** *95*, 562.
(5) Person, M. D.; Kash, P. W.; Butler, L. J. *J. Chem. Phys*. **1992,** *97*, 355.
(6) Tate B. E.; Bartlett, P. E. *J. Am. Chem. Soc*. **1956,** *78*, 5575.
(7) Horwitz, R. J.; Seliskar, C. J.; Guest, J. A., to be published.
(8) Yonezawa H.; Fueno, T. *Bull. Chem. Soc. Jpn*. **1975,** *48*, 22.
(9) Robin, M. B. *Higher Excited States of Polyatomic Molecules;* Academic; New York, 1975; Vol. 2.
(10) Donaldson, D. J.; Gaines, G. A.; Vaida, V. *J. Phys. Chem.* **1988,** *92*, 2766.
(11) Krisher, L. C.; Wilson, E. B. *J. Chem. Phys.* **1959,** *31*, 882.
(12) Sugie, M.; Kuchitsu, K. *J. Mol. Struct*. **1974,** *20*, 437.
(13) Scappini, F.; Dreizler, H. *Z. Naturforsch*. **1976,** *31a*, 840.
(14) Scappini, F.; Mäder, H.; Dreizler, H. *Z. Naturforsch*. **1976,** *31a*, 1398.
(15) Bell, S.; Guirgis, G. A.; Lin, J.; Durig, J. R. *J. Mol. Struct.* **1990,** *238*, 183.
(16) Fisher, W. H.; Carrington, T.; Filseth, S. V.; Sadowski, C. M.; Dugan, C. H. *Chem. Phys*. **1983**, *82*, 443.
(17) Frisch, M. J.; Trucks, G. W.; Head-Gordon, M.; Gill, P. M. W.; Wong, M. W.; Foresman, J. B.; Johnson, B. G.; Schlegel, H. B.; Robb, M. A.; Replogle, E. S.; Gomperts, R.; Andres, J. L.; Raghavachari, K.; Binkley, J. S.; Gonzalez, C.; Martin, R. L.; Fox, D. J.; DeFrees, D. J.; Baker, J.; Stewart, J. J. P.; Pople, J. A. GAUSSIAN92, Revision A; Gaussian, Inc.: Pittsburgh, PA, 1992.
(18) Schlegel, H. B. *J. Comput. Chem.* **1982,** *3*, 214.
(19) Pople, J. A.; Head-Gordon, M.; Fox, D. J.; Raghavachari, K.; Curtis, L. A. *J. Chem. Phys*. **1989,** *90*, 5622.
(20) Curtis, L. A.; Raghavachari, K.; Trucks, G. W.; Pople, J. A. *J. Chem. Phys.* **1991,** *94*, 7221.
(21) Huber K. P.; Herzberg, G. *Molecular Spectra and Molecular Structure;* Van Nostrand Reinhold; New York, 1979; Vol. 4.
(22) Herzberg, G. *Molecular Spectra and Molecular Structure*; Van Nostrand; Princeton, NJ, 1950; Vol. 1.
(23) Brocklehurst, B.; Hebert, G. R.; Innanen, S. H.; Seel R. M.; Nicholls, R. W. *Identification Atlas of Molecular Spectra*; Toronto, 1972, Vol. IX.
(24) Corney, A. *Atomic and Laser Spectroscopy*; Oxford: New York, 1977.
(25) Chase, M. W.; Davies, C. A.; Downey, J. R.; Frurip, D. J.; McDonalds R. A.; Syverud, A. N. *J. Phys. Chem. Ref. Data* **1985**, *14*, Suppl. 1 (*JANAF Thermochemical Tables*, 3rd ed.).
(26) Huang, Y.; Barts S. A.; Halpern, J. B. *J. Phys. Chem.* **1992,** *96*, 425.
(27) Niiranan, J. T.; Gutman D.; Krasnoperov, L. N. *J. Phys. Chem.* **1992,** *96*, 5881.
(28) Fang, W. H.; Liu, R. Z.; You, X. Z. *Chem. Phys. Lett*. **1994,** *226*, 453.
(29) Wiberg, K. B.; Hadad, C. M.; Rablen, D. R.; Cioslowski, J. *J. Am. Chem. Soc.* **1992,** *114*, 8644.
(30) Sugie, M.; Fukiyama, T.; Kuchitsu, K. *J. Mol. Struct.* **1972,** *14*, 333.
(31) Kuchitsu, K.; Fukiyama, T.; Morino, Y. *J. Mol. Struct.* **1969,** *4*, 41.
(32) Watkins, K. W.; Word, W. *Int. J. Chem. Kinet.* **1974,** *6*, 855.
(33) Sears, T. J.; Fawzy W. M.; Johnson, P. M. *J. Chem. Phys.* **1992,** *97*, 3996.
(34) Tuck, A. F. *J. Chem. Soc., Faraday Trans. 2* **1977,** *73*, 689.
(35) Zamir E.; Levine, R. D. *Chem. Phys. Lett.* **1979**, *67*, 237.